

To cite this article: Bhounsule, Pranav A., and Zamani, Ali. "Stable bipedal walking with a swing-leg protraction strategy." *Journal of Biomechanics* 51 (2017): 123-127.

Stable bipedal walking with a swing-leg protraction strategy

Short Communication

Pranav A. Bhounsule and Ali Zamani

Dept. of Mechanical Engineering, University of Texas San Antonio,

One UTSA Circle, San Antonio, TX 78249, USA.

Corresponding author: pranav.bhounsule@utsa.edu

Abstract

In bipedal locomotion, swing-leg protraction and retraction refer to the forward and backward motion, respectively, of the swing-leg before touchdown. Past studies have shown that swing-leg retraction strategy can lead to stable walking. We show that swing-leg protraction can also lead to stable walking. We use a simple 2D model of passive dynamic walking but with the addition of an actuator between the legs. We use the actuator to do full correction of the disturbance in a single step (a one-step dead-beat control). Specifically, for a given limit cycle we perturb the velocity at mid-stance. Then, we determine the foot placement strategy that allows the walker to return to the limit cycle in a single step. For a given limit cycle, we find that there is swing-leg protraction at shallow slopes and swing-leg retraction at steep slopes. As the limit cycle speed increases, the swing-leg protraction region increases. On close examination, we observe that the choice of swing-leg strategy is based on two opposing effects that determine the *time from mid-stance to touchdown*; the walker speed at mid-stance and the adjustment in the step length for one-step dead-beat control. When the walker speed dominates, the swing-leg retracts but when the step length dominates, the swing-leg protracts. This result suggests that swing-leg strategy for stable walking depends on the model parameters, the terrain, and the stability measure used for control. This novel finding has a clear implication in the development of controllers for robots, exoskeletons, and prosthetics and to understand stability in human gaits.

Keywords: Swing-leg Retraction, Walking Stability, Poincaré Map, Dead-beat Control, Locomotion

1 Introduction

It has been observed that during humans walking and running, the swing leg moves backward (the angle between the legs is decreasing) prior to touchdown. This is referred to as ‘swing-leg retraction’ and is hypothesized to stabilize human gait (Daley and Usherwood, 2010; Seyfarth et al., 2003; Wisse et al., 2005).

Model studies of un-actuated machines walking downhill, also known as passive dynamic walking robots (Garcia et al., 1998; McGeer, 1990), have two families of solutions for certain ramp slopes. One solution is stable while the other is unstable. Quite interestingly, the stable solution has a swing-leg retraction while the unstable solution has a swing-leg protraction. This observation led (Wisse et al., 2005) to hypothesize that swing-leg retraction helps improve walking stability. Model studies with controlled swing-leg retraction motions have strengthened this hypothesis. In particular, swing-leg retraction has been demonstrated to increase the stability as measured by the eigenvalue of the Poincaré map (Wisse et al., 2005; Hobbelen and Wisse, 2008), and to increase the ability to reject disturbance (e.g., terrain variation) (Hobbelen and Wisse, 2008). Swing-leg retraction has also been shown to increase the stability and the robustness to disturbances for models of running (Blum et al., 2010; Karssen et al., 2011).

In addition, there have been a number of model-based studies that have tried to understand the benefits of swing-leg retraction beyond stabilization. Specifically, swing-leg retraction has been shown to: (1) increase the energy-efficiency by reducing the foot velocity just before touchdown and by reducing the push-off impulse (Hasaneini et al., 2013b,a; Karssen et al., 2011); (2) minimize foot slippage (Karssen et al., 2011; Hasaneini et al., 2013b); (3) improve the accuracy of predicting touchdown timing (Bhounsule et al., 2014); (4) decrease peak forces at collisions (Karssen et al., 2011); and (5) increase viability and controllability regimes (Hasaneini et al., 2013b). However, the focus of this paper is on the effect of swing-leg strategy on locomotion stability.

How does swing-leg retraction improve walking stability? We provide an explanation based on the paper by (Wisse et al., 2005). Consider a 2D biped model moving with a certain speed, the nominal speed, which corresponds to a certain energy, the nominal energy, (see Fig. 1A). The nominal values above are evaluated at a particular instance in the walking motion (e.g., at mid-stance). Let us assume that the biped speed/energy has changed (e.g., due to a disturbance). In the explanation given below, we are interested in the change in speed, energy, step length, and time with respect to their nominal values.

- (1) When the biped is going fast, it has excess energy. This energy can be dissipated by taking a longer step to get back to the nominal speed (see Fig. 1B). This is because an increase in step length (assuming all other factors are held the same) increases the collisional losses (Ruina et al., 2005), thereby eliminating the excess energy. Similarly, when the biped is going slow, the step length needs to decrease to get back to the nominal speed (see Fig. 1C). *Thus changes in the biped speed and step length have a positive correlation.*
- (2) When the biped is going fast, the step time will decrease. Similarly, when the biped is going slow, the step time will increase. *Thus changes in the biped speed and step time have a negative correlation.*

From (1) and (2) we see that the step length has a negative correlation with the step time which implies a swing-leg retraction strategy (see Fig. 1D). Thus it seems that only swing-leg retraction can lead to stable walking.

However, we argue that (2) is not always true. This is because the step time depends on; (a) the biped speed, and (b) the step length found in (1). When the biped is going fast, the step length needs to increase to get back to the nominal speed as stated in (1). A faster speed will lead to a decrease in the step time but the corresponding increase in step length will increase the step time. When the effect of biped speed dominates the computation of step time, there is swing-leg retraction (see Fig. 1D). But when the effect of step length dominates the computation of step time, there is swing-leg protraction (see Fig. 1E).

Swing-leg protraction can be advantageous because it decreases the energetic cost of swinging the leg. Note that in swing-leg retraction, the hip actuator needs to do more work to move the leg beyond its normal step length so that the swing leg has enough time to be able to move backward before touchdown. However, in swing-leg protraction the leg is moving forward before touchdown and the actuator does not need to do extra work to move the leg beyond its normal step length. Thus, the finding that swing-leg protraction helps bipedal stability has implication for the energy-efficient control of artificial legs in robots, exoskeletons, and prosthetics and in understanding mechanics of human gait.

In this paper, we demonstrate that swing-leg protraction can also lead to stable walking and provide an intuitive explanation. Stable walking with swing-leg protraction has also been independently observed by (Safa and Naraghi, 2015) in a similar walking model but without a hip actuator, but it was mostly ignored as a viable strategy for biped stabilization. Although past results suggest swing-leg retraction leads to stable walking, our results do not contradict them. Specifically, we have examined swing-leg strategies on a broader range of walking motions and terrains not covered in the past studies. Our analysis with a simple bipedal model suggests that the choice of swing-leg strategy depends on the model parameters, the terrain, and the

stability measure used for control. Thus, further investigation is needed to understand the role of swing-leg motion in gait stabilization.

2 Methods

We give brief details of the model and methods used to determine the swing leg control strategy. We use a 2-dimensional model of walking shown in Fig. 2 similar to the one used by (Wisse et al., 2005). The model has massless legs of length ℓ and a point-mass M at the hip. Gravity g points downward and the ramp slope is γ . The stance leg makes an angle of θ with the vertically downward direction and the swing leg makes an angle of ϕ with the stance leg. The model has a rotary hip actuator that can control the swing leg relative to the stance leg.

We use a Poincaré map to relate the state of the walker between successive mid-stance positions (see Fig. 3). We define the mid-stance to be the position when the gravity vector is along the stance leg. Given the variables at step i , namely, the mid-stance velocity ($\dot{\theta}_i^m$), the swing leg angle at touchdown (ϕ_i^-), and the ramp slope (γ), we can find the mid-stance velocity at step $i + 1$ ($\dot{\theta}_{i+1}^m$) using the mapping function F as follows: $\dot{\theta}_{i+1}^m = F(\dot{\theta}_i^m, \phi_i^-, \gamma)$. A limit cycle is the steady state motion of the model. To compute the limit cycle, we put $\dot{\theta}_{i+1}^m = \dot{\theta}_i^m = \dot{\theta}_0^m$, $\phi_i^- = \phi_0$, and $\gamma = \gamma^*$ to get

$$\dot{\theta}_0^m = F(\dot{\theta}_0^m, \phi_0, \gamma^*). \quad (1)$$

See supplementary material for elaborate details on evaluation of F .

Stability is defined as the ability of the biped to stick to the same limit cycle in the presence of a disturbance (e.g., terrain variation, a push). We use the following definition of stability in this analysis: *a limit cycle is stable if the biped can fully correct a perturbation in the state in a single step and unstable otherwise*. Such a controller that allows for full correction of disturbances in a single step is known as one-step dead-beat control (Antsaklis and Michel, 2006). We call this the superstability-based measure. However, the more widely used stability measure is based on the maximum eigenvalues of F , which we call the eigenvalue-based measure. According to the eigenvalue-based measure, the biped is considered to be stable if the magnitude of the maximum eigenvalue is less than 1, and unstable otherwise (Garcia et al., 1998; Strogatz, 1994). The main advantage of our measure, the superstability-based measure over the eigenvalue-based measure, is that it is not based on linearization but is more stringent. Note that both these stability

measures assess the local stability based on small perturbations as opposed to global stability, which is the ability not to fall down under small as well as large perturbations.

We state the control problem as follows. Given a mid-stance velocity at step i , $\dot{\theta}_i^m \neq \dot{\theta}_0^m$, for the given ramp slope, γ^* , we need to find the step length, ϕ_i , required to get back to the nominal mid-stance velocity, $\dot{\theta}_0^m$, at the next step. Thus

$$\dot{\theta}_0^m = F(\dot{\theta}_i^m, \phi_i, \gamma^*). \quad (2)$$

We also need to evaluate the time from mid-stance to touchdown, t_i , which is given as follows

$$t_i = \int_0^{\theta_i^-} \frac{d\theta}{\dot{\theta}} = \int_0^{0.5\phi_i + \gamma^*} \frac{d\theta}{\sqrt{(\dot{\theta}_i^m)^2 + 2(1 - \cos \theta)}} \quad (3)$$

Our numerical calculations are done as follows. To evaluate the limit cycle, we fix the mid-stance speed, $\dot{\theta}_0^m$, and ramp slope, γ , and compute the step length using Eqn. 1. Next, we set $\dot{\theta}_i^m = \dot{\theta}_0^m$ in Eqn. 3 to compute the time from mid-stance to touchdown. Then we vary the mid-stance velocity, $\dot{\theta}_i^m$, and evaluate the swing leg angle, ϕ_i , that will lead to a one-step dead-beat control using Eqn. 2 and the time from mid-stance to touchdown using Eqn. 3.

3 Results and Discussion

We show results for two limit cycles in Fig. 4; $\dot{\theta}_0^m = 0.1$ and $\dot{\theta}_0^m = 0.4$. Figs. 4, A and C, show plots of hip angle at touchdown, ϕ_i^- , vs mid-stance velocity, $\dot{\theta}_i^m$, for various ramp slopes. These plots demonstrate that for faster mid-stance velocity than the nominal, the walker needs to take a longer step than the nominal to get back to the limit cycle, and vice versa for slower mid-stance velocity. The reason is that a longer step length increases while shorter step length decreases the relative energy loss at touchdown (Ruina et al., 2005). Figs. 4, B and D, show plots of the hip angle at touchdown, ϕ_i^- , vs time to touchdown, t_i , as a function of ramp slope. These plots give the trajectory that the swing leg should follow to enable a one-step dead-beat control. That is, if the swing leg follows the specific curve for the given ramp slope, then the biped is guaranteed to return to the limit cycle on the following step.

The gradient at the limit cycle for the plot of swing leg angle versus time (limit cycle shown by the black

dot in Fig. 4) determines the swing-leg strategy; a negative gradient indicates swing-leg retraction while a positive gradient indicates swing-leg protraction. The region of swing-leg protraction is indicated in gray in Fig. 4. Table 1 gives the swing-leg speed for each limit cycle considered in Fig. 4. From the table and the figure we note the following: (1) swing-leg protraction at shallow ramp slopes and swing-leg retraction at steep ramp slopes, and (2) swing-leg protraction region increases as the limit cycle speed increases, that is, the gray region increases with $\dot{\theta}_0^m$. We explain this observation next. The equation for the stance leg is classical inverted pendulum equation and is given by $\ddot{\theta} = \sin \theta$. We do the small angle approximation to rewrite this equation, $\ddot{\theta} = \theta$. Next, we solve this equation and use the initial conditions at mid-stance, $\theta(0) = 0$ and $\dot{\theta}(0) = -\dot{\theta}_i^m$, to get, $\theta(t) = \dot{\theta}_i^m \sinh(t)$. At touchdown we have, $t = t_i$ and $\theta(t_i) = 0.5\phi_i$, thus,

$$\phi_i = 2\dot{\theta}_i^m \sinh t_i. \quad (4)$$

We take the differential of the above equation to get $\partial\phi_i = 2 \sinh t_i (\partial\dot{\theta}_i^m) + 2\dot{\theta}_i^m \cosh t_i (\partial t_i)$. Rearranging the equation, we get the following expression for the swing-leg speed,

$$\frac{\partial\phi_i}{\partial t_i} = \frac{2 \frac{\partial\phi_i}{\partial\dot{\theta}_i^m} \dot{\theta}_i^m \cosh t_i}{\frac{\partial\phi_i}{\partial\dot{\theta}_i^m} - 2 \sinh t_i} \quad (5)$$

The sign of the swing-leg speed depends on the term $\frac{\partial\phi_i}{\partial\dot{\theta}_i^m} - 2 \sinh t_i$ because all the other terms in the expression are positive. From Figs. 4, A and C, we note that $\frac{\partial\phi_i}{\partial\dot{\theta}_i^m}$ at the limit cycle (black dot) is positive but the value decreases as the ramp slope increases. That is, at shallow ramp slopes, the gradient, $\frac{\partial\phi_i}{\partial\dot{\theta}_i^m}$, is large, which makes the denominator in the above equation positive, leading to swing-leg protraction. However, as the ramp slope increases, the gradient $\frac{\partial\phi_i}{\partial\dot{\theta}_i^m}$, is small, which makes the denominator negative, leading to swing-leg retraction. Further, we note that as the limit cycle speed ($\dot{\theta}_m^0$) increases, we get a larger range of ramp slopes where the gradient, $\frac{\partial\phi_i}{\partial\dot{\theta}_i^m}$, is large, thus increasing the swing-leg protraction region (compare the gray region in D with that in B).

The transition from swing-leg retraction to swing-leg protraction occurs through infinity. From Figs. 4, B and D, we note that at shallow ramp slopes, there is swing leg protraction indicated by positive gradient. As the ramp slope increases, the gradient increases, reaching positive infinity. Further increase in the ramp slope causes the gradient to flip from positive to negative infinity and then increases to a finite negative

value. Thus, for each limit cycle speed, $\dot{\theta}_m^0$, there is ramp slope, γ , at which $\frac{\partial \phi_i}{\partial \dot{\theta}_m^0} - 2 \sinh t_i = 0$. When this happens, the swing leg speed is infinite (see Eqn. 5). The physical explanation for this is that the change in leg angle and the change in speed produce an equal and opposite effect on the time from mid-stance to touchdown. Thus, the time from mid-stance to touchdown is unchanged leading to an infinite swing leg speed. As infinite speeds are impossible, the biped loses its ability to be super-stable at this point.

The plot of $\phi_i^-(t_i)$ shown in Figs. 4, B and D can be used to control the hip actuator in exoskeletons and legged robots. When the swing leg is made to follow the $\phi_i^-(t_i)$ trajectory, there will be a complete cancellation of perturbation in speed in a single step, assuming that there are no further disturbances from mid-stance to touchdown. Note that to be able to choose a particular trajectory one requires measurements of mid-stance position, mid-stance speed, and the ramp slope.

One interesting question is that: do humans do one-step dead-beat control under perturbations? By the eigenvalue-based stability metric, this would correspond to a maximum eigenvalue of 0. Past studies on humans show that eigenvalues of walking are between 0.4 and 1 (Dingwell and Kang, 2007), which suggests an exponential decay rather than dead-beat control. But because human walking data is noisy and has considerable variability, even if humans did a dead-beat control (in some dimensions), it would not be distinguishable from an exponential decay.

We assumed that the swing leg is massless in our model. But real robots and humans have legs with finite mass. So the question is to whether the results hold true when the legs are massy. The effect of a massy leg is that the swing leg will add/remove energy during the swing phase, in addition to that at touchdown. However, since robots and humans have relatively light legs (legs account for 15% of human weight (Srinivasan, 2006)), we speculate that adding legs to the model would not alter the results significantly.

4 Conclusions

For a simple 2D point mass model of walking descending a ramp slope there are stable gaits with both, swing-leg retraction as well as swing-leg protraction. The reason for different strategies is because the change in time (compared to nominal step time) from mid-stance to touchdown depends on two opposing effects; the perturbed mid-stance speed and the adjustment in step length. When the speed of walking dominates the computation of the time, we obtain swing leg retraction strategy, but when the step length dominates, we obtain swing-leg protraction strategy. For a given limit cycle characterized by a mid-stance speed, swing-leg protraction stabilizes walking at shallow ramp slopes and swing-leg retraction stabilizes walking at steep

ramp slopes. The swing-leg protraction region increases as the limit cycle speed increases.

Our analysis suggests that the swing-leg strategy depends on the ramp slope, the nominal walking speed, and the definition of stability, which in our case is full cancellation of perturbations in a single step. Thus it is clear that the swing-leg strategy to stabilize bipedal walking is quite complex as it depends on a variety of factors. Further research is needed to elucidate the nature of swing-leg strategy for different models, actuation schemes, and stability specification (e.g., eigenvalue-based stability).

Conflict of Interest

The authors declare that there are no conflicts of interest associated with this work.

References

- Antsaklis, P., Michel, A., 2006. *Linear Systems*, 2nd ed. Birkhauser, Boston, MA.
- Bhounsule, P. A., Cortell, J., Grewal, A., Hendriksen, B., Karssen, J. D., Paul, C., Ruina, A., 2014. Low-bandwidth reflex-based control for lower power walking: 65 km on a single battery charge. *The International Journal of Robotics Research*, 33(10), 1305 – 1321.
- Blum, Y., Lipfert, S., Rummel, J., Seyfarth, A., 2010. Swing leg control in human running. *Bioinspiration & Biomimetics*, 5(2), 1–11.
- Daley, M. A., Usherwood, J. R., 2010. Two explanations for the compliant running paradox: reduced work of bouncing viscera and increased stability in uneven terrain. *Biology Letters*, 6(3), 418–421.
- Dingwell, J. B., Kang, H. G., 2007. Differences between local and orbital dynamic stability during human walking. *Journal of Biomechanical Engineering*, 129(4), 586–593.
- Garcia, M., Chatterjee, A., Ruina, A., Coleman, M., 1998. The simplest walking model: Stability, complexity, and scaling. *ASME Journal of Biomechanical Engineering*, 120(2), 281–288.
- Hasaneini, S. J., Macnab, C. J., Bertram, J. E., Leung, H., 2013a. Optimal relative timing of stance push-off and swing leg retraction. In *Proceedings of 2013 IEEE/RSJ International Conference on Intelligent Robots and Systems*, Tokyo, Japan.

- Hasaneini, S. J., Macnab, C. J., Bertram, J. E., Ruina, A., 2013b. Seven reasons to brake leg swing just before heel strike. In *Dynamic Walking*, Pittsburgh, PA.
- Hobbelen, D. G., Wisse, M., 2008. Swing-leg retraction for limit cycle walkers improves disturbance rejection. *IEEE Transactions on Robotics*, 24(2), 377–389.
- Karssen, J. D., Haberland, M., Wisse, M., Kim, S., 2011. The optimal swing-leg retraction rate for running. In *Proceedings of 2011 IEEE International Conference on Robotics and Automation*, Shanghai, China.
- McGeer, T., 1990. Passive dynamic walking. *The International Journal of Robotics Research*, 9(2), 62–82.
- Ruina, A., Bertram, J., Srinivasan, M., 2005. A collisional model of the energetic cost of support work qualitatively explains leg sequencing in walking and galloping, pseudo-elastic leg behavior in running and the walk-to-run transition. *Journal of Theoretical Biology*, 237(2), 170–192.
- Safa, A. T., Naraghi, M., 2015. The role of walking surface in enhancing the stability of the simplest passive dynamic biped. *Robotica*, 33(1), 195–207.
- Seyfarth, A., Geyer, H., Herr, H., 2003. Swing-leg retraction: a simple control model for stable running. *Journal of Experimental Biology*, 206(15), 2547–2555.
- Srinivasan, M., 2006. Why walk and run: energetic costs and energetic optimality in simple mechanics-based models of a bipedal animal. PhD thesis, Cornell University.
- Strogatz, S., 1994. *Nonlinear Dynamics and Chaos: With Applications to Physics, Biology, Chemistry, and Engineering*. Addison-Wesley, New York, NY.
- Wisse, M., Atkeson, C., Kloimwieder, D., 2005. Swing leg retraction helps biped walking stability. In *Proceedings of 2005 IEEE-RAS International Conference on Humanoid Robots*, Tsukuba, Japan.

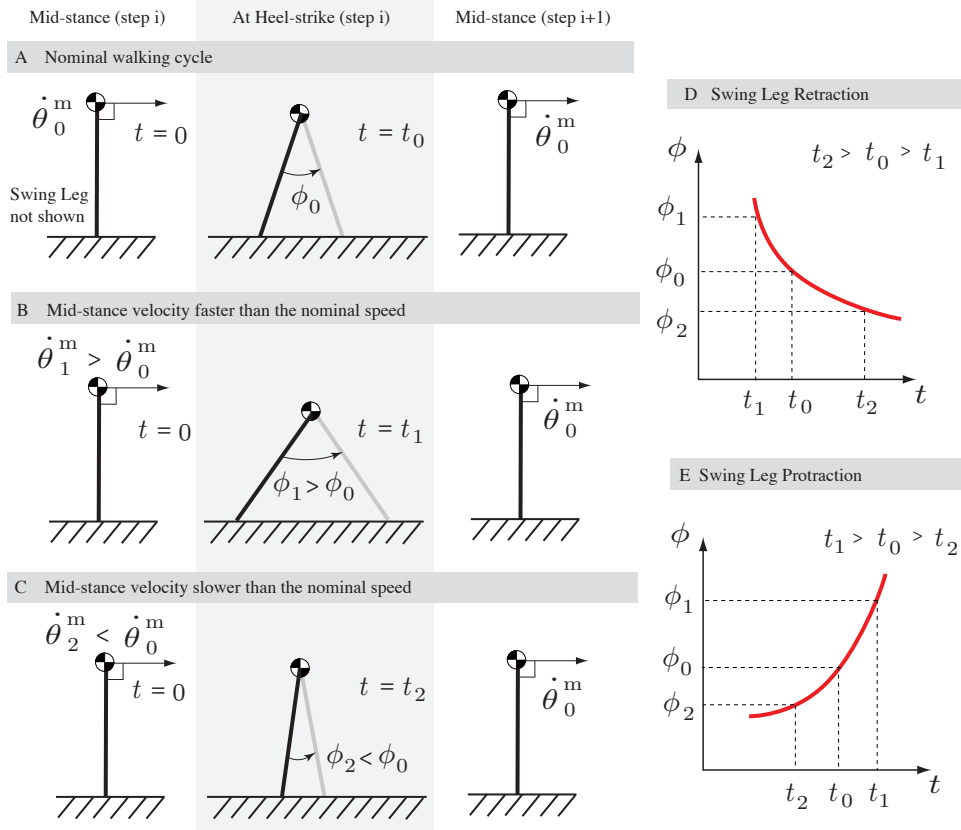


Fig. 1: Hypothetical example to explain swing leg strategy to enable one-step dead-beat control. (A) Nominal walking cycle. The biped has the same mid-stance leg velocity $\dot{\theta}_0^m$ between steps. The nominal step length is ϕ_0 and time from mid-stance to touchdown is t_0 . (B) The biped starts with mid-stance velocity higher than the nominal speed. The biped needs to take a longer than nominal step length $\phi_1 > \phi_0$ to increase the collisional loss compared with the nominal gait to get to the nominal mid-stance velocity of $\dot{\theta}_0^m$. The time in this case is $t = t_1$. (C) The biped starts with mid-stance velocity lower than the nominal speed. The biped needs to take a shorter than nominal step length $\phi_2 < \phi_0$ to reduce the collisional loss compared with the nominal gait to get to the nominal mid-stance velocity of $\dot{\theta}_0^m$. The time in this case is, $t = t_2$. The swing-leg strategy depends on the timing t_1 and t_2 relative to t_0 as discussed next. (D) When the times are such that, $t_2 > t_0 > t_1$, the swing leg needs to retract in order to regulate walking speed. This is indicated by the negative gradient on the ϕ vs t plot. The literature has ample examples of this scenario. (E) When the times are such that, $t_1 > t_0 > t_2$, the swing leg needs to protract in order to regulate the walking speed. This is indicated by the positive gradient on the ϕ vs t plot.

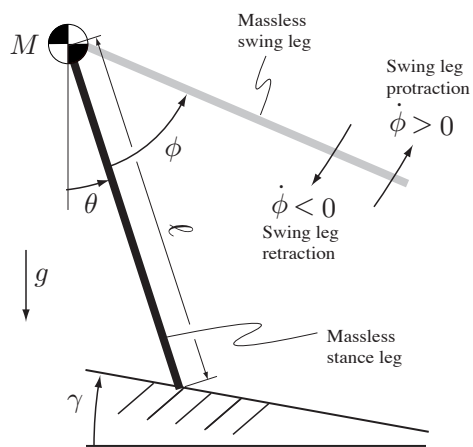


Fig. 2: 2-D point-mass walking model. The walker consists of two massless legs of length ℓ with a point-mass M at the hip joint. Gravity points down and is denoted by g . The stance leg (the leg which is on the ground is shown in black) makes an angle θ with the vertically downward direction. The swing leg (the leg which is in the air is shown in light grey) makes an angle ϕ with the stance leg. We assume that at least one leg is on the ground (single stance phase) and at no instance are both legs on the ground (no double stance phase). The ramp slope is γ . There is an actuator at the hip joint.

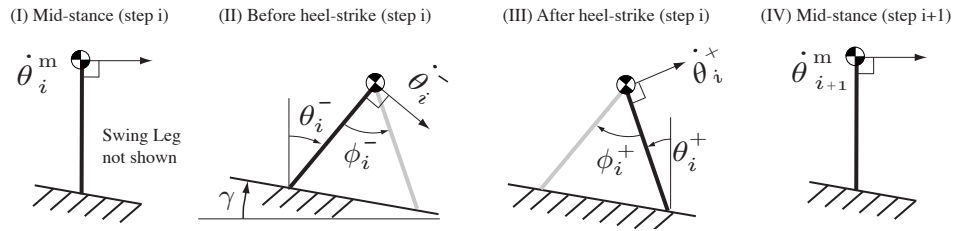


Fig. 3: A typical step of our point mass model. The walker starts in the upright or mid-stance position in (I). In this position, the gravity (not shown in the figure) is along the stance leg and in the downward direction. The swing leg is not shown in I. Next, the stance leg (shown in dark color throughout) moves passively under gravity and the swing leg (shown in light gray color throughout) is controlled to follow a time-based trajectory $\phi(t)$. Just before touchdown in (II), the swing leg is at an angle ϕ_i^- . Next, after touchdown in (III), the swing leg becomes the new stance leg. Finally, the stance leg and the swing leg move passively. The walker ends in the upright position or mid-stance position on the next step in (IV).

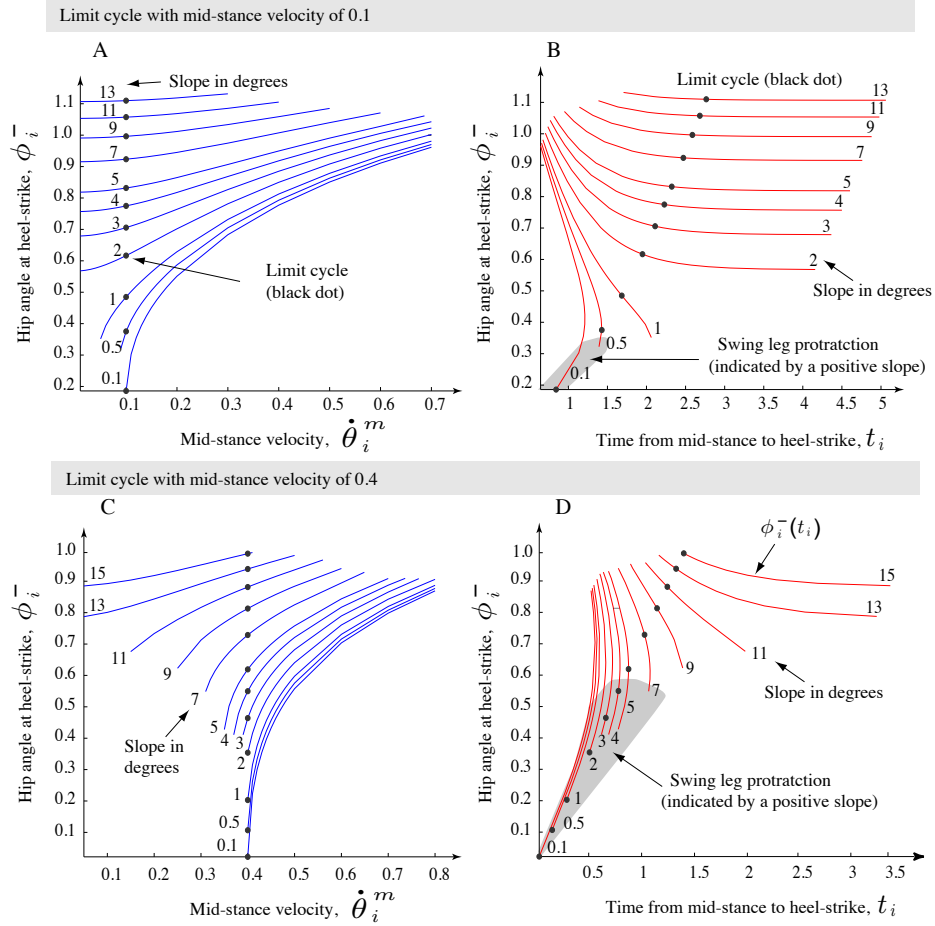


Fig. 4: Swing-leg strategy for two limit cycles for a range of ramp slopes. Plots for the limit cycle characterized with mid-stance velocity $\dot{\theta}_0^m = 0.1$ (A and B) and $\dot{\theta}_0^m = 0.4$ (C and D). The plots on the left column, A and C, show the hip angle at touchdown (ϕ_i^-) vs mid-stance velocity ($\dot{\theta}_i^m$) while the plots on the right column, B and D, show the hip angle at touchdown (ϕ_i^-) vs the time from mid-stance to touchdown (t_i). The model chooses a swing-leg protraction strategy in the grey region and a swing-leg retraction strategy elsewhere.

Table 1: Swing-leg speed for the two limit cycles shown in Fig. 4.

Slope	Swing-leg speed for $\dot{\theta}_0^m = 0.1$	Swing-leg speed for $\dot{\theta}_0^m = 0.4$
0.1	0.4028	0.8342
0.5	-4.5973	0.8630
1.0	-0.3080	0.9212
2.0	-0.1021	1.1352
3.0	-0.0581	1.6134
4.0	-0.0392	3.1871
5.0	-0.0287	-31.1363
7.0	-0.0177	-1.1934
9.0	-0.0121	-0.5580
11.0	-0.0088	-0.3458
13.0	-0.0066	-0.2418

Stable bipedal walking with a swing-leg protraction strategy
Supplementary material

Pranav A. Bhounsule and Ali Zamani

Corresponding author: pranav.bhounsule@utsa.edu,

Dept. of Mechanical Engineering, University of Texas San Antonio,

One UTSA Circle, San Antonio, TX 78249, USA.

1 Bipedal model and equations of motion

A figure of the model and a single step of the model are shown in Fig. 2 and Fig. 3 respectively, in the paper. The step starts in the mid-stance phase (stance leg is along the gravitational field) at step i and ends in the mid-stance phase at step $i + 1$. We present the equations of motion next.

1.1 Mid-stance position at step i (Fig. 3 , I) to instant before touchdown at step i (Fig. 3 , II)

The non-dimensional mid-stance velocity at step i is $\dot{\theta}_i^m$. We have non-dimensionalised the time with $\sqrt{\ell/g}$. From (I) to (II), the stance leg moves passively to the instant before touchdown, while the swing leg is controlled by the hip actuator to follow a time-based trajectory $\phi(t)$. In (II), the instant before touchdown, the stance leg makes an angle of θ_i^- with the vertical, the swing leg makes an angle of ϕ^- with the stance leg, and the non-dimensional stance leg velocity is $\dot{\theta}_i^-$.

Since the swing leg is massless, it does not affect the motion of the stance leg. Hence, we may apply energy conservation from (I) to (II) to get

$$\frac{(\dot{\theta}_i^m)^2}{2} + 1 = \frac{(\dot{\theta}_i^-)^2}{2} + \cos \theta_i^-. \quad (1)$$

Let non-dimensional ground reaction force be R (non-dimensionalized with Mg). Since the legs are massless, R acts along the stance leg. Using Newton's law we derive an expression for R . Further, the leg

can only push against the ground. Hence the reaction R needs to be positive. Thus

$$R = \cos \theta - \dot{\theta}^2 \geq 0. \quad (2)$$

The angular speed, $\dot{\theta}_i$, increases monotonically as the angle θ_i increases with time. Thus, we check for the condition given by (2) only during touchdown (i.e., when the vertical angle is at its maximum after mid-stance). Thus

$$\cos \theta_i^- \geq (\dot{\theta}_i^-)^2. \quad (3)$$

Substituting $\dot{\theta}_i^-$ from Eqn. 1 in Eqn. 3 and simplifying, we get

$$\cos \theta_i^- \geq \frac{(\dot{\theta}_i^m)^2 + 2}{3}. \quad (4)$$

Let t_i be the time it takes for the walker to move from mid-stance position to the instant just before touchdown. Then

$$t_i = \int_0^{\theta_i^-} \frac{d\theta}{\dot{\theta}} = \int_0^{\theta_i^-} \frac{d\theta}{\sqrt{(\dot{\theta}_i^m)^2 + 2(1 - \cos \theta)}} \quad (5)$$

which we solve using numerical quadrature.

1.2 Instant before touchdown at step i (Fig. 3 , II) to instant after touchdown at step i (Fig. 3 , III)

At touchdown, the legs form a closed loop with the ramp. This condition is given by

$$\cos(\theta_i^- - \phi_i^-) - \cos(\theta_i^-) + 2 \sin\left(\frac{\phi_i^-}{2}\right) \sin \gamma = 0. \quad (6)$$

At touchdown, we switch the angles of the stance and swing legs. To find the angular velocity of the stance leg after touchdown $\dot{\theta}_i^+$, we do an angular momentum balance about the impending collision point

(Garcia et al., 1998)

$$\theta_i^+ = \theta_i^- - \phi_i^-, \quad (7)$$

$$\phi_i^+ = -\phi_i^-, \quad (8)$$

$$\dot{\theta}_i^+ = \dot{\theta}_i^- \cos \phi_i^-. \quad (9)$$

1.3 Instant after touchdown at step i (Fig. 3 , III) to mid-stance position at step $i + 1$ (Fig. 3 , IV)

Let the mid-stance velocity at step $i + 1$ be $\dot{\theta}_{i+1}^m$. Because the legs are massless, we may use the conservation of energy to relate the energy of the point mass between III and IV

$$\frac{(\dot{\theta}_{i+1}^m)^2}{2} + 1 = \frac{(\dot{\theta}_i^+)^2}{2} + \cos \theta_i^+. \quad (10)$$

We also need to ensure that the ground reaction force is positive from III to IV. Using an argument similar to that used to derive Eqn. 3, we get

$$\cos \theta_i^+ \geq (\dot{\theta}_i^+)^2. \quad (11)$$

Next, we substitute $(\dot{\theta}_i^+)^2$ from Eqn. 10 and θ_i^+ from Eqn. 7 into Eqn. 11 and simplify to get

$$\cos(\theta_i^- - \phi_i^-) \geq \frac{(\dot{\theta}_{i+1}^m)^2 + 2}{3}. \quad (12)$$

2 Methods

To analyze the walking motion we use tools in dynamical systems, namely Poincaré Map and Limit Cycles.

2.1 Poincaré Map

The Poincaré map is used to analyze walking motions of this model as done by others (Garcia et al., 1998; McGeer, 1990). To compute the map, we need to relate the state of the walker at any instant in the step with the same instant on the next step. Here, we will relate the state at mid-stance of the current step, i , (see Fig. 3 (I)) to the mid-stance at the next step, $i + 1$ (see Fig. 3 (IV)). To do this, we can use Eqns. 1,

6, 7, 8, 9, and 10. These 6 equations have 9 variables; $\dot{\theta}_i^m$, $\dot{\theta}_{i+1}^m$, $\dot{\theta}_i^+$, $\dot{\theta}_i^-$, θ_i^+ , θ_i^- , ϕ_i^+ , ϕ_i^- , and γ . We can use the 6 equations to eliminate 5 variables to end up with an equation with 4 independent variables,

$$\dot{\theta}_{i+1}^m = F(\dot{\theta}_i^m, \phi_i^-, \gamma), \quad (13)$$

where the Poincaré map F , is a scalar function that maps the state $(\dot{\theta}_i^m)$ from mid-stance at step, i , to the state at the next step $(\dot{\theta}_{i+1}^m)$, $i + 1$, for a given step length ϕ_i^- , and ramp slope γ .

2.2 Limit Cycle

Limit cycles are periodic solutions of the Poincaré map F . To do this, we need to find a fixed point of the function F . Since we want to find solution for a given ramp slope, we fix the slope $\gamma = \gamma^*$ in Eqn. 13 and try to find the step length $\phi_i^- = \phi_0$ that will lead to $\dot{\theta}_{i+1}^m = \dot{\theta}_i^m = \dot{\theta}_0^m$. Using the variables above, we can rewrite Eqn. 13 as

$$\dot{\theta}_0^m = F(\dot{\theta}_0^m, \phi_0, \gamma^*). \quad (14)$$

2.3 One-step dead-beat control

A controller that does full correction of disturbances in a single step is known as a one-step dead-beat control (Antsaklis and Michel, 2006). We state the one-step dead-beat control as follows. For the disturbance that leads to a mid-stance velocity at step i , $\dot{\theta}_i^m \neq \dot{\theta}_0^m$, for the given terrain γ^* , we have to find the step length ϕ_i , needed to get back to the nominal mid-stance velocity $\dot{\theta}_0^m$ at the next step. Thus

$$\dot{\theta}_0^m = F(\dot{\theta}_i^m, \phi_i, \gamma^*). \quad (15)$$

2.4 Numerical evaluation of limit cycles and dead-beat control

Our prime goal is to compute the step length ϕ_i vs time t_i for a given limit cycle. We proceed as follows. Each limit cycle is characterized by a specified mid-stance velocity. Thus, the mid-stance velocity at the next step is given, $\dot{\theta}_{i+1}^m = \dot{\theta}_0^m$. The ramp slope is given, $\gamma = \gamma^*$. Next, for a range of mid-stance velocities, $0 < \dot{\theta}_i^m < 1$, we find values of the 6 unknowns $\dot{\theta}_i^+$, $\dot{\theta}_i^-$, θ_i^+ , θ_i^- , ϕ_i^+ , and ϕ_i^- using the 6 equations, Eqns. 1, 6, 7, 8, 9, and 10. Also, we rule out solutions that violate the take-off conditions given by Eqns. 4 and 12. We can also compute the time to go from mid-stance to touchdown, t_i , using Eqn. 5 using the computed

values of θ_i^- and $\dot{\theta}_i^m$. Further, we repeat the above calculation for a range of ramp slopes, $0.01^\circ < \gamma^* < 15^\circ$. Beyond 15° there are no walking solutions (Bhounsule, 2014).

References

- Antsaklis, P., Michel, A., 2006. Linear Systems, 2nd ed. Birkhauser, Boston, MA.
- Bhounsule, P., 2014. Foot placement in the simplest slope walker reveals a wide range of walking motions. IEEE Transactions on Robotics., 30(5), 1255 – 1260.
- Garcia, M., Chatterjee, A., Ruina, A., Coleman, M., 1998. The simplest walking model: Stability, complexity, and scaling. ASME Journal of Biomechanical Engineering, 120(2), 281–288.
- McGeer, T., 1990. Passive dynamic walking. The International Journal of Robotics Research, 9(2), 62–82.